– Supporting Information –

Dissociation of the K-Ras4B/PDEδ Complex upon Contact with Lipid Membranes: Membrane Delivery Instead of Extraction

Katrin Weise,[†] Shobhna Kapoor,[†] Alexander Werkmüller,[†] Simone Möbitz,[†] Gunther Zimmermann,[‡, §] Gemma Triola,[‡, §] Herbert Waldmann,[‡, §] and Roland Winter*[,†]

[†] Physical Chemistry I - Biophysical Chemistry, Faculty of Chemistry, TU Dortmund University, Otto-Hahn-Strasse 6, D-44227 Dortmund, Germany

[‡] Department of Chemical Biology, Max Planck Institute of Molecular Physiology, Otto-Hahn-Strasse 11, D-44227 Dortmund, Germany

[§] Chemical Biology, Faculty of Chemistry, TU Dortmund University, Otto-Hahn-Strasse 6, D-44227 Dortmund, Germany

Corresponding Author

E-mail: roland.winter@tu-dortmund.de

MATERIALS AND METHODS

Materials and sample preparation. The phospholipids 1,2-dioleoyl-*sn*-glycero-3-phosphocholine (DOPC), 1,2-dioleoyl-*sn*-glycero-3-phospho-(1'-*rac*-glycerol) sodium salt (DOPG), 1,2-dipalmitoyl-*sn*-glycero-3-phospho-(1'-*rac*-glycerol) sodium salt (DPPG), and 1,2-dipalmitoyl-*sn*-glycero-3-phosphocholine (DPPC) were purchased from Avanti Polar Lipids (Alabaster, AL). Cholesterol (Chol), 4-(2-hydroxyethyl)piperazine-1-ethanesulfonic acid (Hepes), octyl β-D-glucopyranoside, guanidine hydrochloride, and 3-[(3-cholamidopropyl)dimethylammonio]-1-propanesulfonate (Chaps) were from Sigma Aldrich (Deisenhofen, Germany). Magnesium chloride, tris(hydroxymethyl)-aminomethan (Tris), and chloroform were obtained from Merck (Darmstadt, Germany); bovine serum albumin (BSA) from Pierce (Bonn, Germany). The fluorescent lipid *N*-(lissamine rhodamine B sulfonyl)-1,2-dihexadecanoyl-*sn*-glycero-3-phosphoethanolamine triethylammonium salt (*N*-Rh-DHPE) and 4,4-difluoro-5,7-dimethyl-4-bora-3a,4a-diaza-*s*-indacene-3-propionic acid, succinimidyl ester (BODIPY-FL, SE) were from Molecular Probes (Invitrogen). The extruder and suitable polycarbonate membranes (0.1 µm) as well as filter supports were purchased from Avanti Polar Lipids (Alabaster, AL); larger membrane filters (0.2 µm) were obtained from GE Healthcare (Munich, Germany).

Stock solutions of 10 mg mL^{-1} lipid (DOPC, DOPG, DPPC, DPPG, and Chol) in chloroform/methanol 4:1 for DPPG and chloroform for all other lipids were prepared and mixed to obtain 1.94 mg of total lipid with the desired composition of DOPC/DPPC/Chol 25:50:25 (molar ratio), DOPC/DOPG/DPPC/DPPG/Chol 20:5:45:5:25 for AFM, SPR, and fluorescence spectroscopy experiments, and DOPC/DOPG/DPPC/DPPG/Chol 15:10:40:10:25 for fluorescence anisotropy measurements. After removal of the solvent by drying under vaccum overnight, the dry lipids were resuspended in 1 mL of 10 mM Hepes, 5 mM $MgCl_2$, 150 mM NaCl, pH 7.4 for the SPR or 20 mM Tris, 7 mM $MgCl_2$, pH 7.4 for the AFM and fluorescence spectroscopy experiments to yield a total lipid concentration of 3 mM. For the fluorescence anisotropy measurements, lipid films were resuspended in 0.5 mL of 10 mM Tris, 5 mM $MgCl_2$, pH 7.4, yielding a higher lipid concentration of 6 mM to avoid dilution effects upon addition of the lipid solution to the protein measured before. Details on the formation of large unilamellar vesicles (LUVs) of 100 nm size by extrusion can be found in refs. S1–S3. The extruded lipid solution was further diluted to a concentration of 0.5 mM for the SPR experiments.

Protein synthesis. The synthesis of the K-Ras4B proteins is described in detail in ref. S4. Briefly, the *S*-farnesylated K-Ras4B protein was synthesized by a combination of expressed protein ligation (EPL) and lipopeptide synthesis. The K-Ras4B peptide, possessing an additional cysteine at the N-terminus required for protein ligation, with the amino acid sequence H-Cys(S*t*Bu)-Lys_6-Ser-Lys-Thr-Lys-Cys(Far)-OMe was synthesized on a 2-chlorotrityl resin. After cleavage from the solid support, the peptide was purified and ligated to a truncated K-Ras4B protein core thioester that was generated via expression in Impact™ vector pTWIN2 (New England Biolabs) and subsequent transformation of the resulting plasmid into *E. coli* BL21(DE3) cells. This yields a ligated K-Ras4B protein bearing an additional cysteine between Gly^{174} and Lys^{175}. The truncated K-Ras4B thioester was labeled with BODIPY or dansyl prior to ligation by adding a 10× excess of either BODIPY-NHS or dansyl to the K-Ras4B thioester buffered in a 100 mM solution of $NaHCO_3$, pH 8.5 and shaking at 4°C for 3 h under argon. For the synthesis of the K-Ras4B GTP, a nucleotide exchange step was introduced after BODIPY labeling of the protein core thioester. Subsequent ligation of the GTP-loaded K-Ras4B protein core thioester to the corresponding peptide yielded the desired K-Ras4B GTP protein.[S3] His6-tagged PDEδ was expressed as described previously.[S5] For $Arl2^{GTP}$, the bound nucleotide was exchanged for GppNHp by the addition of a fivefold excess of GppNHp in the presence of alkaline phosphatase and incubation overnight. Afterwards, the buffer was exchanged and the nucleotide content was determined by HPLC.[S13]

Surface plasmon resonance (SPR). SPR experiments were carried out with a Biacore 3000 system (Biacore, Uppsala, Sweden). For the protein-membrane interaction studies, the pioneer L1 sensor chip (GE Healthcare, Munich, Germany) was used that is composed of a thin lipophilic modified dextran matrix on a gold surface, upon which lipid bilayers can be immobilized through the capture of liposomes by the lipophilic compounds.[S1,S6] The chip has been shown to be suitable for the generation of model membrane systems that provide a flexible lipid bilayer surface that closely resembles the surface of a cellular membrane.[S7,S8] All measurements were carried out at a temperature of 25°C, with the samples cooled at 10°C in the autosampler before the measurement was started.

Prior to the experiment, the L1 chip was primed 4× with Hepes buffer (10 mM Hepes, 5 mM $MgCl_2$, 150 mM NaCl, pH 7.4). Afterwards, the chip surface underwent a cleaning program by injecting 30 µL 2-propanol / 50 mM NaOH (2:3), 10 µL octyl β-D-glucopyranoside (40 mM), and 30 µL Chaps (20 mM), NaCl (100 mM), and $CaCl_2$ (20 mM) at a flow rate of 5 µL/min. For vesicle immobilization, 15 µL of the extruded lipid vesicle solution (0.5 mM) were injected twice at a flow rate of 2 µL/min, which was followed by a stabilization phase by injecting 50 µL of Hepes buffer at a flow rate of 100 µL/min and three further injec-

tions of 10 µL 25 mM NaOH at a flow rate of 5 µL/min. Finally, the lipid surface was stabilized by injecting 40 µL Hepes buffer at a flow rate of 20 µL/min. For each lipid mixture, a separate flow cell was used. After baseline stabilization, 40 µL of the protein containing solution ($c_{\text{K-Ras4B}}$ = 2 µM, $c_{\text{PDE}\delta}$ = 3.4 µM) were injected at a flow rate of 20 µL/min and the dissociation was followed for 30 min. For the membrane interaction studies with the PDEδ-complexed K-Ras4B, K-Ras4B was mixed with PDEδ prior to injection into the SPR flow cell to yield a final concentration of 2 µM K-Ras4B and 3.4 µM PDEδ. After following the dissociation for 30 min, the chip surface was regenerated using the cleaning program. The degree of chip surface coverage with lipids was determined by means of 0.5 µM BSA and was found to be →75% for all cases.

To eliminate unspecific binding effects such as the interaction of Hepes buffer with the L1 chip and non-specific binding of the proteins to the pure L1 chip that depend on the determined lipid coverage, these signals were subtracted from the actual sensorgrams of the respective protein solutions. Hence, the ratio of the maximal amplitude of the BSA-membrane and BSA-chip sensorgram yields the amount of the chip surface that is not covered with lipids and is used as a factor for correcting the zeroized (i.e., setting the baseline before injection of the protein solution to zero) protein-chip sensorgram. This corrected sensorgram is then subtracted from the buffer-corrected and zeroized protein-membrane sensorgram to yield the final protein-membrane sensorgram for analysis. All sensorgrams were recorded at a frequency of 10 Hz.

For all measurements performed, the SPR data were analyzed on the basis of a multi-step model owing to the non-simple-exponential association and dissociation curves observed in the sensorgrams for the protein-membrane interaction, reflecting a complex interaction behavior. A two-step reaction model was shown to provide an appropriate curve-fitting algorithm and describes a process with two reaction steps that, in terms of protein-lipid interactions, correspond to:

$$\text{P} + \text{L} \underset{k_{\text{off},1}}{\overset{k_{\text{on},1}}{\rightleftharpoons}} \text{PL} \underset{k_{\text{off},2}}{\overset{k_{\text{on},2}}{\rightleftharpoons}} \text{PL}^{*} ,$$

(Scheme 1)

where the soluble protein (P) binds to the immobilized lipids (L) forming a primary binding complex (PL) and a secondary protein-lipid complex (PL*, e.g. a clustered state as shown for K-Ras4B by atomic force microscopy[S3]) after relocation of protein and lipid molecules within the lipid bilayer plane. The effect of the K-Ras4B clustering on the response measured is indirect in altering the equilibrium between the bound and free forms of the protein, allowing a dissociation of PL* only through reversal of the clustering reaction step. To directly obtain values for the association rate constant k_{on}, the whole sensorgram was fitted to the two-step model. The parameters $k_{\text{on},1}$ and $k_{\text{on},2}$ represent the corresponding association rates of the respective reaction steps. Curve fitting was performed by using the Marquardt-Levenberg algorithm and the fitted curves were generated by numerical integration of the differential equations that describe the reaction scheme. This fitting procedure was implemented in the BIAevaluation software 4.1 (Biacore, Uppsala, Sweden). Owing to this complex reaction scheme, the maximum error bars of the fits were sometimes large due to error propagation. Hence, the initial association phase (for $t \rightarrow 0$), which is directly proportional to $k_{\text{on},1}$, was also evaluated by linear regression using Origin 7 (OriginLab Corporation, Northampton, MA, USA), resulting in values for the initial slope of the sensorgram. The model and the corresponding analysis have been described in detail in ref. S1.

Whereas the two-step fit of the whole sensorgram gave reasonable results for the association phase, a larger discrepancy was observed for the fitted dissociation part of the curve. Thus, the dissociation phase was fitted separately to a biexponential model (Eq. 1) using Origin 7, yielding two independent dissociation rate constants $k_{\text{off},1}$ and $k_{\text{off},2}$ as well as their respective contributions A_1 and A_2.

$$R = A_1 \times e^{-k_{\text{off},1}(t-t_0)} + A_2 \times e^{-k_{\text{off},2}(t-t_0)} + \text{offset} \qquad (1)$$

t_0 indicates the beginning of the dissociation phase, i.e., the time point when the flow cell switched from protein to buffer solution. The relative amount of quasi-irreversibly bound protein was derived by correlating the offset value of the biexponential fit to the initial amplitude at the starting point (t = 0) of the dissociation phase corresponding to the following equation:

$$\text{quasi}-\text{irrevers.} = \frac{\text{offset}}{A_1 + A_2 + \text{offset}} \quad . \qquad (2)$$

From Equation 1, an average dissociation rate $\bar{k}_{\text{diss}}$ can be calculated:

$$\bar{k}_{\text{diss}} = \frac{A_1}{A_1 + A_2} \times k_{\text{off},1} + \frac{A_2}{A_1 + A_2} \times k_{\text{off},2} \quad . \qquad (3)$$

Finally, after determining the association and dissociation rate constants for the two-step binding process, the equilibrium dissociation constant K_{D} can be calculated according to:

$$K_{\text{D}} = \frac{k_{\text{off},1}}{k_{\text{on},1}} \times \frac{k_{\text{off},2}}{k_{\text{on},2}} \quad . \qquad (4)$$

The error bars in all experiments represent the standard deviation from at least four (up to nine) inde-

pendently conducted experiments, and the corresponding values for all determined kinetic parameters are given in Tables S1 and S2.

Atomic force microscopy (AFM). Details of the preparation of the supported lipid bilayers and the AFM setup are described in ref. S2. Briefly, vesicle fusion on mica was carried out by depositing 35 μL of the extruded lipid vesicle solution together with 35 μL of Tris buffer on freshly cleaved mica (NanoAndMore, Wetzlar, Germany) and incubation in a wet chamber at 70 °C for 2 h. For the protein–membrane interaction studies, 200 μL of either K-Ras4B (2 μM), PDEδ (3.4 μM), or K-Ras4B GTP/PDEδ (2 μM / 3.4 μM) in 20 mM Tris, 7 mM $MgCl_2$, pH 7.4 were injected into the AFM fluid cell at room temperature and allowed to incubate for 1 h. Afterwards, the fluid cell was rinsed carefully with Tris buffer before imaging to remove unbound protein.

Measurements were performed on a MultiMode scanning probe microscope with a NanoScope IIIa controller (Digital Instruments, Santa Barbara, CA) and by use of a J-Scanner (scan size 125 μm). Images were obtained by applying the tapping mode in liquid with oxide-sharpened silicon nitride (DNP-S) or sharp nitride lever (SNL) probes mounted in a fluid cell (MTFML, Veeco, Mannheim, Germany). Tips with nominal force constants of 0.32 N m^{-1} were used at driving frequencies around 9 kHz and drive amplitudes between 80 and 550 mV; scan frequencies were between 0.5 and 1.0 Hz.

Infrared reflection absorption spectroscopy (IRRAS). The IRRAS measurements were carried out according to refs. S3 and S9. All experiments were performed with a Wilhelmy film balance (Riegler, Berlin, Germany) using a filter paper as Wilhelmy plate. Two teflon troughs of different sizes were linked by two small bores to ensure equal heights of the air-D_2O interface in both troughs. The temperature of the subphase was maintained at 20 ± 0.5°C and measurements were performed in the small (reference) trough at constant surface area. A Plexiglas hood covered the entire reflection attachment to minimize the evaporation of subphase. Both troughs were filled with 100 mM NaCl in D_2O. Monolayers of DOPC/DOPG/DPPC/DPPG/
Chol 20:5:45:5:25 were formed by directly spreading the lipid solution (1 mM) in a mixture of chloroform and methanol (3:1) onto the subphase. Protein adsorption measurements were performed by premixing PDEδ and K-Ras4B GTP before injection of the protein solution into the aqueous subphase below the lipid monolayers to yield a concentration of K-Ras4B GTP and PDEδ of 200 and 340 nM, respectively.

Infrared spectra were recorded using a Vertex 70 FT-IR spectrometer (Bruker, Germany) connected to an A511 reflection attachment (Bruker) with an MCT detector using the trough system described above. The IR beam is focused by several mirrors onto the subphase and the trough system was positioned on a movable platform to be able to shuttle between sample and reference troughs. This shuttle technique diminishes the spectral interference due to water vapour absorption in the light beam. Parallel polarized light at an angle of incidence of 35° was used for recording of the IRRA spectra. All spectra were recorded at a spectral resolution of 8 cm^{-1} using Blackman-Harris-3-term apodization and a zero filling factor of 2. For each spectrum 2000 scans were co-added. The single beam reflectance spectrum of the big trough was ratioed as background (R_o) to the single beam reflectance spectrum of the lipid monolayer on the reference trough (R) to calculate the reflection absorption spectrum as $-\log(R/R_o)$. For PDEδ, measurements at different angles of incidence using parallel (p) and perpendicular (s) polarized light were performed after reaching a constant surface pressure (equilibrium state). By following the amide-I′ band taken with p-polarized light at varying angles of incidence information on the orientation of the protein at the lipid monolayer interface can be obtained.[S10] The measured IRRA signal can be either positive or negative, depending on the angle of incidence and orientation of the transition dipole moment with respect to the interface. At a given angle of incidence above the Brewster angle, positive absorption intensities imply a transition dipole oriented preferentially in the surface plane, and negative intensities reflect a perpendicular orientation.

Fluorescence anisotropy and spectroscopy. All fluorescence spectroscopy measurements were performed on a K2 multifrequency phase and modulation fluorometer (ISS Inc., Champaign, IL). The temperature was maintained at 25°C and controlled with an accuracy of ±0.1 °C using a circulating water bath. Time-resolved fluorescence lifetime and anisotropy measurements were performed in the frequency-domain using the cross-correlation technique.[S11,S12] By using this technique, the BODIPY-fluorophore was excited with intensity-modulated light resulting in intensity-modulated fluorescence emission. BODIPY-fluorescence was generated by use of a 473 nm laser diode (ISS Inc., Champaign, IL) directly connected to a function generator, yielding modulated excitation light over a frequency range of 2–173 MHz at a cross-correlation frequency of 400 Hz. The BODIPY-emission was collected through a 505 nm long-pass filter. Fluorescence lifetime measurements at magic-angle conditions have been performed prior to the anisotropy experiments. To this end the excitation light was vertically polarized (0°), while the emission polarizer was set to an angle of 54.7°. The fluorescence of BODIPY-FL was used as lifetime reference (5.7 ns in MeOH). In case of the anisotropy experiments, the excitation light was vertically polarized, whereas the

emission was recorded at polarization angles of 0° and 90°. The corresponding phase and modulation data were measured as a function of the modulation frequency. The fluorescence lifetime data were fitted using a model that includes two discrete lifetime components describing the fluorescence intensity decay:

$$I(t) = \alpha_1 \exp(-t/\tau_1) + \alpha_2 \exp(-t/\tau_2)\,, \tag{5}$$

where τ_1 and τ_2 are the fluorescence lifetimes with the corresponding amplitudes α_1 und α_2. From the parameters obtained the average fluorescence lifetime $\langle\tau\rangle$ of the BODIPY-label can be calculated (Table S3):

$$<\tau> = f_1\tau_1 + f_2\tau_2\ , \tag{6}$$

where τ_1 and τ_2 are the fluorescence lifetimes and f_1 and f_2 are the corresponding fractional intensities, which can be calculated from fluorescence lifetimes and their amplitudes by using the following equation:

$$f_i = \alpha_i\tau_i / \sum_i \alpha_i\tau_i\,. \tag{7}$$

Reduced χ^2-values were obtained in a range from 1 to 5.

Differential phase and modulation data of the fluorescence anisotropy experiments were also fitted to a biexponential model:

$$r(t) = r_0\left[g_1 \cdot \exp(-t/\theta_1) + g_2 \cdot \exp(-t/\theta_2)\right]\ , \tag{8}$$

where r_0 is the maximum anisotropy. θ_1 and θ_2 correspond to the reorientational times of the BODIPY-label and are usually related to the segmential motion of the label (θ_1) and the overall rotation of the protein (θ_2, which is thus equivalent to the overall rotational correlation time θ_{protein} of BODIPY-labeled K-Ras4B). The pre-exponential factors g_1 and g_2 are the associated fractional amplitudes ($g_1 + g_2 = 1$; Table S4). During the fitting process, the previously obtained lifetime parameters (τ_1, τ_2, f_1, and f_2) were entered as fixed parameters (cf. Table S3). Reduced χ^2-values were obtained in a range of 1 to 4. Experimental errors in Figure 3 of the manuscript are calculated from repeated measurements and listed separately in Tables S3 and S4.

For the protein measurements in solution, BODIPY-K-Ras4B was diluted with Tris buffer to a final concentration of 1 µM in case of K-Ras4B GDP, and 2 µM for K-Ras4B GTP and truncated K-Ras4B GDP (negative control). First, the lifetime and anisotropy data of these proteins were measured in the absence of PDEδ. Second, PDEδ was subsequently added in a 1.7-fold molar excess to the BODIPY-labeled K-Ras4B, and the solutions were allowed to incubate for 1 h. Finally, anionic raft lipid vesicles were added to the K-Ras4B GTP/PDEδ-solution and allowed to incubate for 1 h, yielding a lipid concentration of 0.6 mM. Lifetime and anisotropy data were determined for K-Ras4B proteins after every incubation step. For studying electrostatic lipid-protein interactions in case of the full-length BODIPY-K-Ras4B GDP, lifetime and anisotropy data were recorded for the protein in Tris buffer and after addition of LUVs composed of either DOPC/DPPC/Chol or DOPC/DOPG/DPPC/DPPG/Chol (final lipid concentration 0.6 mM).

For the PDEδ tryptophan emission experiments, the excitation light at 282 nm was provided by a xenon lamp and the emission spectra were collected at 90° through a monochromator. First, the emission spectrum of PDEδ (6.8 µM) in 20 mM Tris, 7 mM $MgCl_2$, pH 7.4 was collected, followed by the addition of K-Ras4B GTP (4 µM) and finally the anionic raft vesicles were added. The emission spectra for the protein bound to raft vesicles were background corrected for the scattering by the corresponding lipid vesicles.

REFERENCES

(S1) Gohlke, A.; Triola, G.; Waldmann, H.; Winter, R. *Biophys. J.* **2010**, *98*, 2226–2235.

(S2) Weise, K.; Triola, G.; Brunsveld, L.; Waldmann, H.; Winter, R. *J. Am. Chem. Soc.* **2009**, *131*, 1557–1564.

(S3) Weise, K.; Kapoor, S.; Denter, C.; Nikolaus, J.; Opitz, N.; Koch, S.; Triola, G.; Herrmann, A.; Waldmann, H.; Winter, R. *J. Am. Chem. Soc.* **2011**, *133*, 880–887.

(S4) Chen, Y.-X.; Koch, S.; Uhlenbrock, K.; Weise, K.; Das, D.; Gremer, L.; Brunsveld, L.; Wittinghofer, A.; Winter, R.; Triola, G.; Waldmann, H. *Angew. Chem. Int. Ed.* **2010**, *49*, 6090–6095.

(S5) Alexander, M.; Gerauer, M.; Pechlivanis, M.; Popkirova, B.; Dvorsky, R.; Brunsveld, L.; Waldmann, H.; Kuhlmann, J. *ChemBioChem.* **2009**, *10*, 98–108.

(S6) Cooper, M.A.; Hansson, A.; Löfås, S.; Williams, D.H. *Anal. Biochem.* **2000**, *277*, 196–205.

(S7) Besenicar, M.; Macek, P.; Lakey, J.H.: Anderluh, G. *Chem. Phys. Lipids* **2006**, *141*, 169–178.

(S8) Mozsolits, H.; Thomas, W.G.; Aguilar, M.I. *J. Pept. Sci.* **2003**, *9*, 77–89.

(S9) Meister, A.; Nicolini, C.; Waldmann, H.; Kuhlmann, J.; Kerth, A.; Winter, R.; Blume, A. *Biophys. J.* **2006**, *91*, 1388–1401.

(S10) Mendelsohn, R.; Brauner, J.W.; Gericke, A. *Annu. Rev. Phys. Chem.* **1995**, *46*, 305–334.

(S11) Gratton, E.; Limkeman, M. *Biophys. J.* **1983**, *44*, 315–324.

(S12) Gratton, E.; Jameson, D.M.; Hall, R.D. *Annu. Rev. Biophys. Bioeng.* **1984**, *13*, 105–124.

(S13) Kühnel, K.; Veltel, S.; Schlichting, I.; Wittinghofer, A. *Structure.* **2006**, *14*, 367–378.

FIGURES

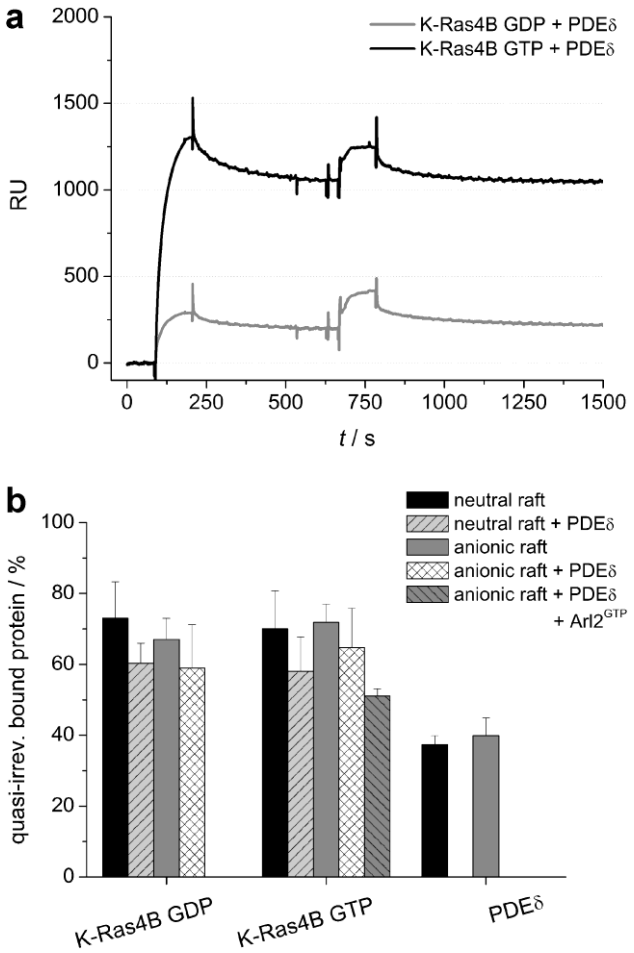

Figure S1. (a) SPR sensorgrams of the membrane binding of GDP- and GTP-loaded K-Ras4B (c = 2 μM) to neutral raft membranes composed of DOPC/DPPC/Chol 25:50:25 (molar ratio) and subsequent addition of PDEδ (c = 3.4 μM). The data show that PDEδ is not able to extract K-Ras4B from neutral raft membranes, independent on Ras nucleotide loading. (b) Summarized SPR data for the relative amount of quasi-irreversibly bound protein at the end of each dissociation phase for GDP- and GTP-loaded K-Ras4B as well as PDEδ and the K-Ras4B/PDEδ-complex in the presence of membranes composed of DOPC/DPPC/Chol 25:50:25 (molar ratio; black) and DOPC/DOPG/DPPC/DPPG/Chol 20:5:45:5:25 (grey). The shaded bars indicate the data for the PDEδ-complexed K-Ras4B. In addition, the effect of $Arl2^{GTP}$ on the PDEδ binding affinity is shown. The error bars represent the standard deviation from 3–9 measurements. All kinetic parameters are given in Tables S1 and S2.

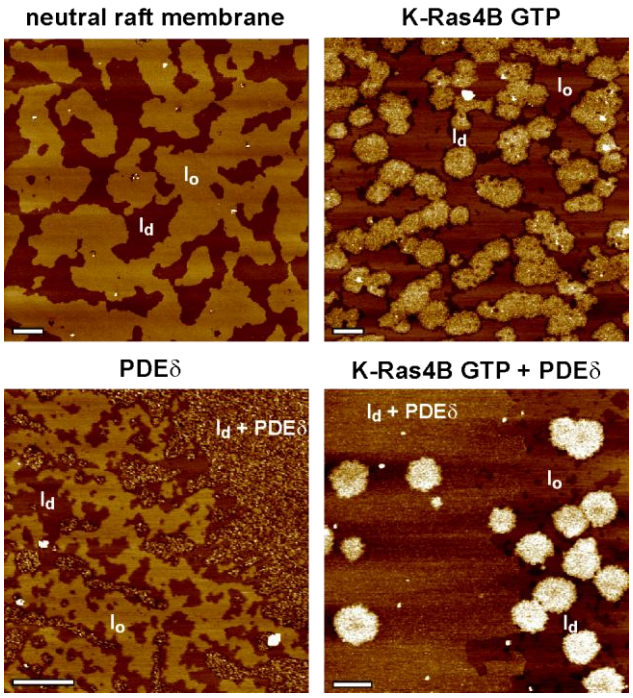

Figure S2. AFM images of the interaction of K-Ras4B GTP, PDEδ, and the preformed K-Ras4B/PDEδ complex with membranes composed of DOPC/DPPC/Chol 25:50:25 (molar ratio). The upper left panel shows a representative AFM image of the neutral raft membrane before injection of 200 μL protein solution ($c_{\text{K-Ras4B}}$ = 2 μM and $c_{\text{PDE}\delta}$ = 3.4 μM) into the AFM fluid cell. The AFM images of K-Ras4B GTP,[S3] PDEδ, and K-Ras4B GTP + PDEδ display the membrane partitioning of the proteins at a particular time point, i.e., at $t \approx 24$ h. The overall height of the vertical color scale from dark brown to white corresponds to 6 nm for all images; the scale bar represents 1 μm.

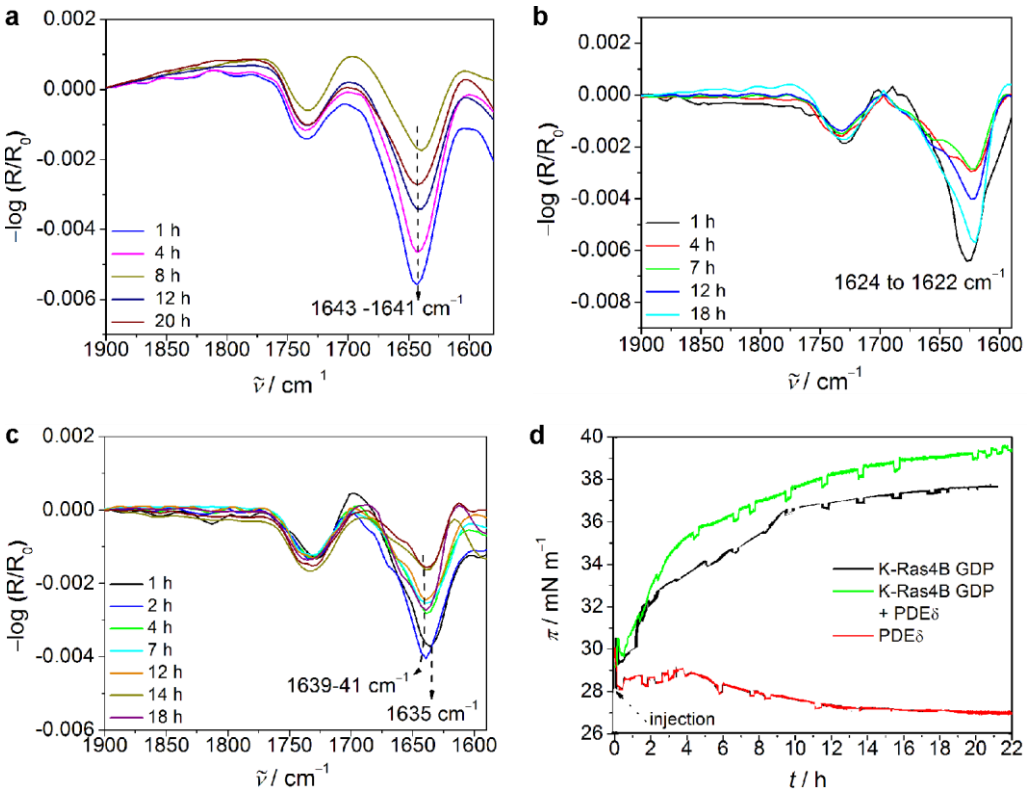

Figure S3. IRRA spectra for (a) K-Ras4B GDP,[S3] (b) PDEδ, and (c) K-Ras4B GDP + PDEδ inserted into or adsorbed at the anionic raft monolayer (kept at ~30 mN m^{-1}) acquired with p-polarized light at 35° angle of incidence. Panel d shows the surface pressure profiles for K-Ras4B GDP (black), PDEδ (red), and K-Ras4B GDP + PDEδ (green) upon interaction with the raft monolayer.

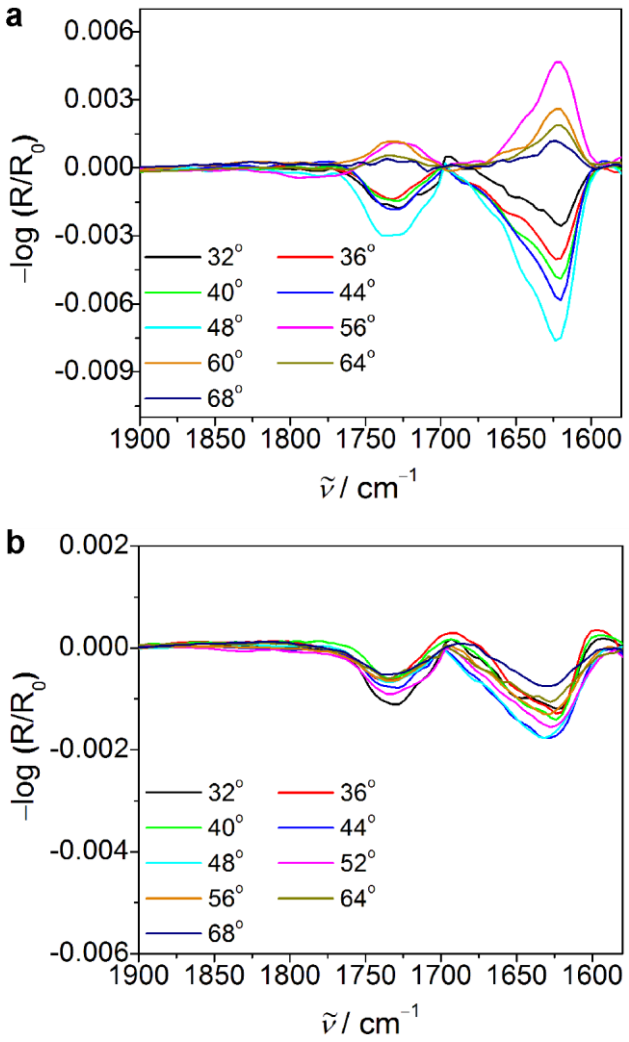

Figure S4. IRRA spectra for PDEδ upon adsorption at the anionic raft monolayer at equilibration with varying angle of incidence from 32 to 68° acquired with (a) p-polarized and (b) s-polarized light.

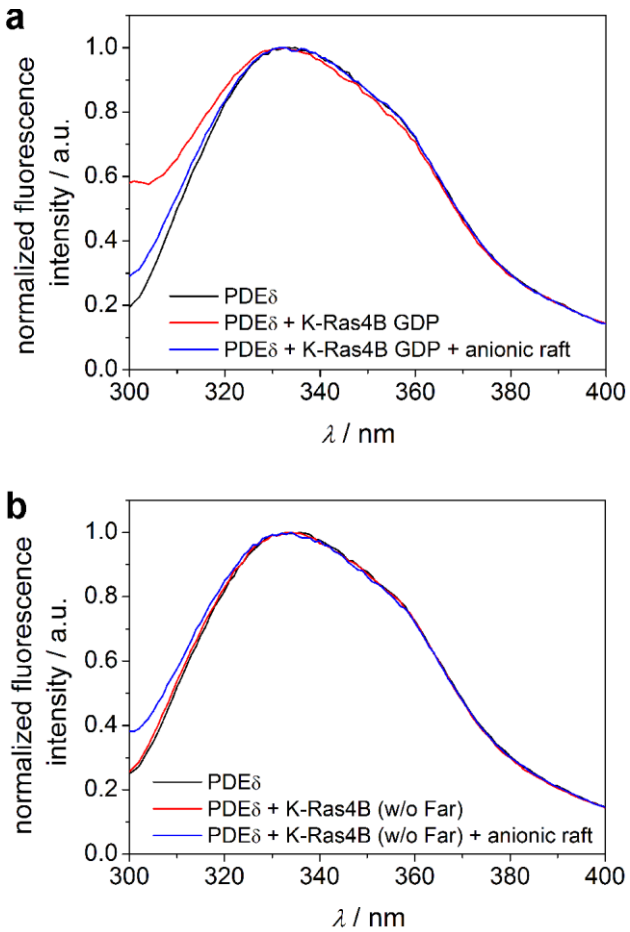

Figure S5. Normalized fluorescence spectra of PDEδ in bulk solution (black), either the K-Ras4B GDP/PDEδ-complex or the complex of unlipidated K-Ras4B and PDEδ in bulk solution (red), and the K-Ras4B GDP/PDEδ-complex or unlipidated K-Ras4B/PDEδ-complex upon interaction with the anionic raft membrane (blue) at 25 °C. The spectra show the change of the PDEδ tryptophan emission maximum and band shape upon complexation and membrane-mediated dissociation of the PDEδ and K-Ras4B GDP complex (a). In contrast, no blue shift of the PDEδ fluorescence spectrum could be detected for the unlipidated K-Ras4B protein (b).

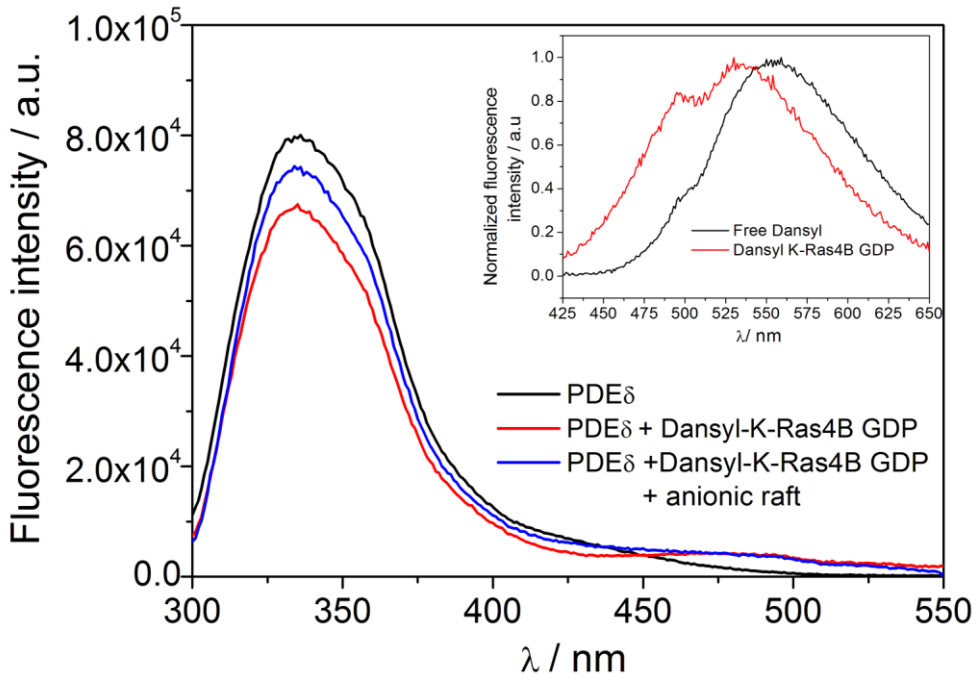

Figure S6. FRET assay of PDEδ binding to Dansyl-labeled K-Ras4B GDP in solution and dissociation from the K-Ras4B GDP upon addition of anionic lipid raft vesicles.

A FRET based assay was conducted with PDEδ–tryptophan as donor and Dansyl-labeled K-Ras4B GDP as acceptor. Dansyl–K-Ras4B GDP (6.8 μM) in the presence and absence of PDEδ (6.8 μM) was excited at λ = 282 nm, and the emission fluorescence spectrum was measured from 300 to 550 nm. The fluorescence spectrum of the mixture of PDEδ and Danysl–K-Ras4B GDP was corrected for the cross excitation signal of the pure Dansyl–K-Ras4B GDP. Significant energy transfer occurred as detected by the increasing fluorescence intensity in the 425–550 nm region (with broad maxima around 494 nm). As expected, quenching of the intrinsic tryptophan fluorescence of PDEδ by Dansyl was observed owing to resonance energy transferred from PDEδ to the fluorescent probe, thereby confirming the complexation of PDEδ with the farnesylated and labeled K-Ras4B GDP. Upon addition of the anionic raft lipid vesicles, the increase in the intrinsic tryptophan fluorescence of PDEδ (after background subtraction of the scattering signal by lipids and cross excitation by pure Dansyl–K-Ras4B GDP) argues for the dissociation of the complex upon membrane contact, leading to reduced FRET, thereby increasing the donor signal, as supported by the other experimental claims. Comparison of the fluorescence spectrum of the free Dansyl group in solution (Dansyl amide) and in complex with K-Ras4B GDP shows a strong blue shift with two overlapping emission maxima centered on 494 nm and 530 nm when excited at 340 nm (Figure S6, inset). Such a broad peak of Dansyl when conjugated with K-Ras4B coupled with the limitation to monitor the emission spectra beyond 550 nm (due to effects of second order monochromator excitation) prevents us from analyzing changes in Dansyl–K-Ras4B fluorescence. Moreover, the inherent low labeling efficiency of the K-Ras proteins also renders the analysis in the acceptor region quite ambiguous. For these reasons, we focus on the FRET-induced changes in the donor region here only, which suffices to answer the question raised.

TABLES

Table S1. Summary of all kinetic parameters of the interaction of GDP- and GTP-loaded K-Ras4B, PDEδ as well as PDEδ-bound GDP- and GTP-loaded K-Ras4B with membranes composed of DOPC/DOPG/DPPC/DPPG/Chol 20:5:45:5:25. In the table, the mean value ± standard deviation (n = 4-9) is given.

	K-Ras4B GDP	K-Ras4B GDP + PDEδ	K-Ras4B GTP	K-Ras4B GTP + PDEδ	PDEδ	K-Ras4B GTP + PDEδ + Arl2^{GTP}
$k_{on,1}$ / M^{-1} s^{-1}	1.15×10^{5} ± 6.68×10^{4}	4.05×10^{4} ± 2.70×10^{4}	1.29×10^{5} ± 1.80×10^{5}	1.13×10^{5} ± 1.36×10^{5}	2.89×10^{4} ± 5.59×10^{3}	4.08×10^{4} ± 8.0×10^{3}
$k_{on,2}$ / s^{-1}	0.01 ± 4.00×10^{-3}	0.02 ± 5.00×10^{-3}	0.02 ± 0.03	0.02 ± 7.00×10^{-3}	0.01 ± 1.00×10^{-3}	4.00×10^{-3} ± 2.00×10^{-3}
$k_{off,1}$ / s^{-1}	0.08 ± 0.06	4.00×10^{-3} ± 4.00×10^{-3}	0.10 ± 0.10	6.00×10^{-3} ± 6.00×10^{-3}	0.02 ± 0.02	0.07 ± 0.05
$k_{off,2}$ / s^{-1}	0.07 ± 0.07	0.01 ± 5.00×10^{-3}	0.04 ± 0.03	0.02 ± 0.02	0.02 ± 0.02	0.03 ± 0.05
$\bar{k}_{diss}$ / s^{-1}	0.08 ± 0.02	8.00×10^{-3} ± 5.54×10^{-4}	0.08 ± 0.06	0.01 ± 5.00×10^{-3}	0.02 ± 6.00×10^{-3}	0.05 ± 0.01
K_D / M	2.62×10^{-6} ± 1.54×10^{-6}	8.67×10^{-8} ± 7.84×10^{-8}	1.95×10^{-5} ± 3.65×10^{-5}	6.06×10^{-8} ± 8.16×10^{-8}	3.33×10^{-7} ± 1.34×10^{-7}	2.72×10^{-6} ± 9.74×10^{-7}
quasi-irrev. bound protein / %	67.01 ± 6.01	59.01 ± 12.19	71.82 ± 5.24	64.76 ± 11.13	39.90 ± 5.00	51.15 ± 2.00
initial slope / RU s^{-1}	14.89 ± 6.22	158.16 ± 22.57	50.94 ± 22.05	227.30 ± 21.23	218.23 ± 28.88	106.84 ± 3.75

Table S2. Summary of all kinetic parameters of the interaction of GDP- and GTP-loaded K-Ras4B, PDEδ as well as PDEδ-bound GDP- and GTP-loaded K-Ras4B with membranes composed of DOPC/DPPC/Chol 25:50:25. In the table, the mean value ± standard deviation (n = 4-8) is given.

	K-Ras4B GDP	K-Ras4B GDP + PDEδ	K-Ras4B GTP	K-Ras4B GTP + PDEδ	PDEδ
$k_{on,1}$ / M^{-1} s^{-1}	$7.39\times10^4 \pm 5.17\times10^4$	$4.80\times10^4 \pm 1.08\times10^4$	$8.03\times10^4 \pm 7.44\times10^4$	$3.73\times10^4 \pm 5.78\times10^3$	$5.60\times10^4 \pm 2.64\times10^4$
$k_{on,2}$ / s^{-1}	$0.01 \pm 6.00\times10^{-3}$	$0.02 \pm 2.00\times10^{-3}$	$0.01 \pm 4.00\times10^{-3}$	$0.02 \pm 3.00\times10^{-3}$	$0.01 \pm 9.94\times10^{-4}$
$k_{off,1}$ / s^{-1}	0.04 ± 0.05	0.03 ± 0.03	0.05 ± 0.04	0.01 ± 0.02	0.03 ± 0.03
$k_{off,2}$ / s^{-1}	0.07 ± 0.05	0.02 ± 0.02	0.04 ± 0.04	0.04 ± 0.03	0.02 ± 0.02
$\bar{k}_{diss}$ / s^{-1}	0.06 ± 0.02	$0.02 \pm 2.00\times10^{-3}$	$0.05 \pm 8.00\times10^{-3}$	$0.02 \pm 7.00\times10^{-3}$	$0.02 \pm 7.00\times10^{-3}$
K_D / M	$2.13\times10^{-6} \pm 1.69\times10^{-6}$	$3.26\times10^{-7} \pm 3.11\times10^{-7}$	$1.91\times10^{-6} \pm 2.28\times10^{-6}$	$4.14\times10^{-7} \pm 1.93\times10^{-7}$	$3.50\times10^{-7} \pm 4.98\times10^{-8}$
quasi-irrev. bound protein / %	73.09 ± 10.24	60.27 ± 5.74	70.03 ± 10.79	58.01 ± 9.79	37.38 ± 2.51
initial slope / RU s^{-1}	105.01 ± 15.27	100.66 ± 6.29	89.04 ± 11.96	117.40 ± 3.62	182.46 ± 18.91

Table S3. Results of the fluorescence lifetime analysis: The average fluorescence lifetime $\langle\tau\rangle$ was calculated from the corresponding fluorescence lifetimes τ_1 and τ_2 of BODIPY-labeled K-Ras4B and the accordant fractional intensities f_1 and f_2. In the table, the mean value ± standard deviation is given.

	f_1	τ_1 / ns	f_2	τ_2 / ns	$\langle\tau\rangle$ / ns
K-Ras4B GDP trunc.	0.04 ± 0.01	1.10 ± 0.04	0.96 ± 0.01	5.68 ± 0.01	5.49 ± 0.07
K-Ras4B GDP	0.07 ± 0.03	1.57 ± 0.44	0.93 ± 0.03	5.80 ± 0.78	5.51 ± 0.04
K-Ras4B GDP trunc. + PDEδ	0.03 ± 0.01	1.32 ± 0.05	0.97 ± 0.01	5.72 ± 0.02	5.58 ± 0.02
K-Ras4B GTP	0.04 ± 0.01	2.06 ± 0.56	0.96 ± 0.01	5.97 ± 0.07	5.81 ± 0.03
K-Ras4B GTP + PDEδ	0.08 ± 0.01	1.77 ± 0.75	0.92 ± 0.01	5.78 ± 0.08	5.48 ± 0.04
K-Ras4B GDP + neutral raft	0.08 ± 0.04	1.22 ± 0.26	0.92 ± 0.04	5.69 ± 0.09	5.31 ± 0.22
K-Ras4B GDP + anionic raft	0.06 ± 0.01	1.06 ± 0.33	0.94 ± 0.01	5.72 ± 0.08	5.44 ± 0.04
K-Ras4B GTP + PDEδ + anionic raft	0.05 ± 0.01	0.97 ± 0.10	0.95 ± 0.01	5.58 ± 0.10	5.36 ± 0.09

Table S4. Results of the fluorescence anisotropy analysis: Rotational correlation times θ_1 and θ_2 (with θ_2 being equal to the overall rotational correlation time of the protein, i.e., $\theta_2 = \theta_{protein}$) of BODIPY-labeled K-Ras4B and corresponding fractional amplitudes g_1 and g_2. In the table, the mean value ± standard deviation is given.

	g_1	θ_1 / ns	g_2	θ_2 / ns	r_0
K-Ras4B GDP trunc.	0.61 ± 0.04	0.55 ± 0.05	0.39 ± 0.01	12.80 ± 1.13	0.28 ± 0.01
K-Ras4B GDP	0.47 ± 0.01	1.13 ± 0.25	0.53 ± 0.01	14.95 ± 0.78	0.30 ± 0.01
K-Ras4B GDP trunc. + PDEδ	0.61 ± 0.01	0.53 ± 0.02	0.39 ± 0.01	12.85 ± 1.63	0.28 ± 0.01
K-Ras4B GTP	0.45 ± 0.01	0.98 ± 0.08	0.55 ± 0.01	12.64 ± 0.20	0.33 ± 0.01
K-Ras4B GTP + PDEδ	0.46 ± 0.02	1.04 ± 0.18	0.54 ± 0.01	21.05 ± 3.04	0.35 ± 0.02
K-Ras4B GDP + neutral raft	0.45 ± 0.01	1.32 ± 0.22	0.55 ± 0.01	17.25 ± 0.49	0.29 ± 0.01
K-Ras4B GDP + anionic raft	0.39 ± 0.01	1.29 ± 0.25	0.61 ± 0.01	24.45 ± 4.60	0.31 ± 0.01
K-Ras4B GTP + PDEδ + anionic raft	0.39 ± 0.02	0.81 ± 0.25	0.61 ± 0.01	22.73 ± 4.22	0.36 ± 0.03